



ELSEVIER

March 1995

Materials Letters 22 (1995) 265-270

**MATERIALS
LETTERS**

Ultrasound-processed silica xerogels behavior during heating

E. Blanco, M. Ramírez-del-Solar, N. de la Rosa-Fox, L. Esquivias

Departamento de Estructura y Propiedades de los Materiales, University of Cádiz, Apartado 40, 11510 Puerto Real, Cádiz, Spain

Received 6 September 1994; in final form 2 December 1994; accepted 6 December 1994

Abstract

Silica formamide-containing xerogels were prepared by different processing methods in order to evaluate sonocatalysis and solvent effects on xerogel thermal evolution. Characterization of the evolution of the xerogels upon heating was carried out by means of different thermal analysis techniques. The results offer valuable information for the selection of the proper thermal paths in order to obtain adequate materials for different xerogel applications. From the evaluation of the thermal features a mechanism of the formamide desorption from xerogel surface is proposed.

1. Introduction

The sol-gel route for materials processing is based on the formation of a porous solid network (gel) by the aggregation of particles of a sol. Gel densification occurs at relatively low temperatures leading to a final material with different shapes and structures, depending on the manufacturing circumstances [1]. Rapid and reliable production of gel monoliths is necessary to implement many of the potential advantages of this ultrastructure processing of materials. Nevertheless, the gel is immersed in a residual liquid, arising from the sol preparation, which must be eliminated beforehand, by adequate heat treatments, in order to have a dried gel. Frequently, gels are obtained by hydrolysis and polycondensation of metal alkoxides in the presence of a catalyst and a common solvent, usually an alcohol, required to obtain a homogeneous solution.

One of the problems of maintaining the gel's monolithic quality comes from capillary stress which develops during the evacuation of the liquid from the pores, making the gel crack [2]. It has been demonstrated that some surface active organics, added as co-solvent in the sol preparation, are very useful for rapid drying

without cracking. One of these chemicals, known as drying control chemical additive (DCCA), is the formamide. This product has a substantial influence on the reaction rates leading to a hard gel with large and uniform pore size, decreasing its capillary pressure gradient and increasing its toughness compared to those gels prepared without DCCA [3]. On the other hand, several studies have been undertaken by our group in order to elucidate the potential of solventless processing accomplished by subjecting the alkoxide-water mixture to intense ultrasonic radiation [4,5]. The structure and visco-elastic behavior of the resulting sonogels differ from the 'classic gel', synthesized in the presence of a solvent, and depend very much on the insonation dose which becomes, in this way, a new kinetic parameter.

In view of the potential value of ultrasound and DCCA for tailoring gel structures for particular applications, it is important to evaluate the effect of both agents on the behavior of the gel during the early stages of the heat treatment when they act simultaneously. A precise knowledge of the temperature range required to eliminate the remaining unwanted chemical residues is essential in order to design the sintering step to obtain

a very pure and homogeneous final product. With this aim, a systematic thermal study of silica gels prepared by different procedures has been undertaken using several techniques, the results of which are presented in this paper.

2. Sample preparation

Hydrolysis of tetraethoxysilane (TEOS) was accomplished by the addition of 10 mol H₂O/mol TEOS, the pH of which had been previously adjusted to 1 with nitric acid. Formamide, used as DCCA, was added in a molar ratio $R_f=7$. Gels with this composition were prepared, for comparison, by three different procedures.

Sonogels were obtained by subjecting the two-phases water + formamide/TEOS mixture to the action of 20 kHz high power ultrasonic radiation. The ultrasound processor had 600 W as power output and a standard horn with a 13 mm tip. The insonation dose was limited for the minimum dose required for the hydrolysis to start and that for which ‘in situ’ gelation takes place during the ultrasonic action. Minimum and maximum values were found to be, respectively, ≈ 0.07 and 0.34 kJ/cm³, from an earlier calibration of the system as described in a previous paper [6]. In this energy density range, two different samples were prepared with 0.1 and 0.3 kJ/cm³, designated as low (LF7) and high (HF7) dose samples.

In a second solventless method, a clear solution results because of the alcohol generated during the hydrolysis reaction of the mixture induced by mechanical stirring. This sample was labeled as 0F7.

Finally, the classic method of dissolving both phases in a specific volume of ethanol (50% volume of TEOS) was followed for the preparation of the sample coded as EF7. Sols resulting from the four different processes were poured in hermetically closed polyethylene containers and kept in an electric oven at 40°C for gelation. Gelation time was checked as an indication of the influence of the experimental procedure on the kinetic reactions. It was defined as the elapsed time at 40°C at the moment when, tilting the container, no more fluidity was observed. Measured values were 5, 70 and 200 min for the HF7, LF7 and 0F7, respectively. In the case of the classic sample (EF7), gelation time was longer than one day.

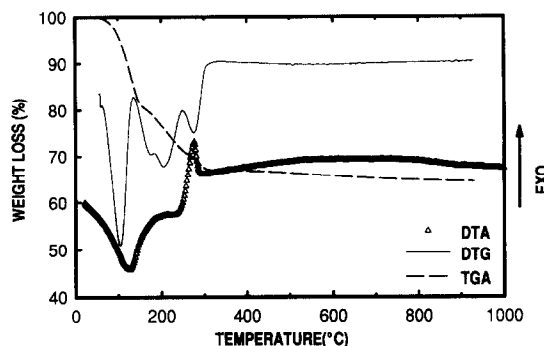


Fig. 1. TGA curves of the sonogel obtained with the higher ultrasonic dose (HF7). DTA of the same sample is also compared in the figure with the thermogravimetric derivative. Notice the occurrence of five steps during the decomposition process of the xerogels.

Gels were aged for 7 days and dried at 40°C, keeping the container opened, until the syneresis liquid was completely removed. After this treatment, the gel volume reduction due to shrinkage was around 15%. Finally, aging was completed in the oven at 100°C for 24 h.

3. Thermal characterization

The temperature evolution of these different xerogels, once they were stabilized at 100°C, was studied using four different analysis techniques. Thermogravimetric and differential thermal analysis (TGA and DTA) and differential scanning calorimetry (DSC) were carried out on the samples, in nitrogen atmosphere with a Perkin-Elmer TGA7, DTA 1700 and DSC-7, respectively. Thermal programmed decomposition (TPD) experiments, that are further explained below, were also carried out. All the experiments were accomplished at a constant heating rate (10°C/min). Previous analyzer calibrations were performed from the onset temperature and peak area corresponding to several standards: melting point of indium, lead and tin for DSC analyzer, melting point of gold and lead for the DTA equipment and perkalloy and zinc Curie point temperature for the TG analyzer.

Fig. 1 shows the TGA and DTA curves of the HF7 sample. Similar profiles were obtained for the other samples. The derivative thermogram (DTG) has also been included in order to clarify the onset and final temperature of each process. Peak positions and shapes in the derivative curves indicate that an overlapping

Table 1
Xerogels mass loss (in wt%) at five heating steps

Sample	100°C	140–160°C	200°C	290°C	300–800°C
HF7	20	6	4	4	3
LF7	21	3	5	4	3
OF7	21	2	4	3	3
EF7	15	3	5	4	3

reaction occurs. Then, for a more precise calculation of the mass change from the area under the peaks, deconvolution of them was performed by an extrapolation procedure. From the DTG curves, five different steps can be discerned: the first one centered at 100°C, the second one at 200°C with a shoulder in the 140–160°C range, an additional step at 290°C and a spread band from 300 to 800°C, which corresponds to the last TGA curve step. Percentages of the mass losses, calculated from the thermograms in these five steps, are presented in Table 1 for all the samples. The results point out that the most important loss takes place during the first step, at around 100°C. If we consider that before the experiment was performed these samples were stabilized at 100°C and after exposure to the atmosphere, the initial mass loss must be related to desorption of atmospheric water physically retained on the xerogel surface.

DTA diagrams exhibit two peaks: a wide endothermic one from room temperature to $\approx 170^\circ\text{C}$ and a sharp exothermic one centered at 290°C. From the temperature position, we presume that they correspond to the thermograms of the two first steps and the fourth one, respectively.

The DSC curves are represented in Fig. 2 in the 50–350°C temperature range, normalized for the same sample quantity. Notice the presence of two main peaks. The endothermic peak, at around 140–165°C agrees with the shoulder observed at 160°C in the DTG and DTA diagrams. In agreement with the DTA results, DSC plots also present an exothermic peak (260–290°C) which must be related with the fourth TGA step observed during the thermal decomposition.

Table 2 summarizes the enthalpy data obtained, from the area of the DSC peaks, for all the processes and

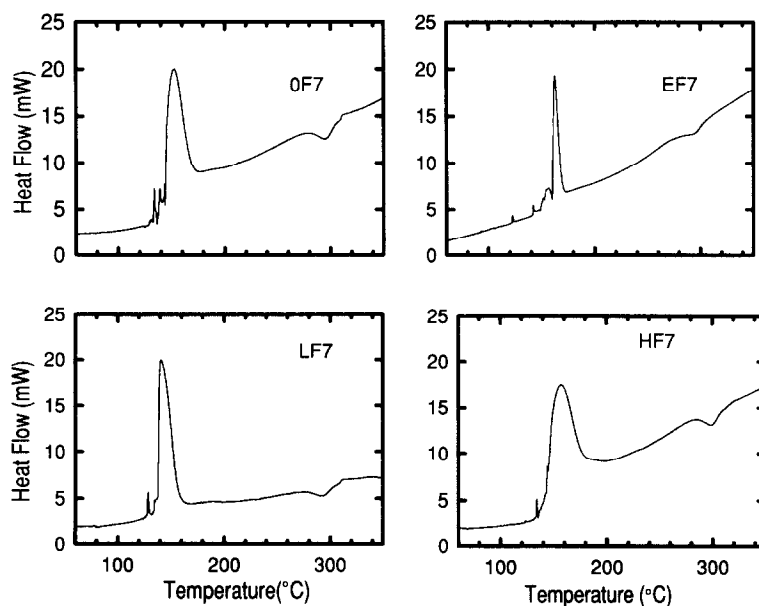


Fig. 2. DSC plots for all the samples, stabilized at 100°C, in which, in agreement with DTA results, two peaks are shown: OF7, EF7, LF7, HF7. Data are represented in arbitrary units with the upward direction indicating an exothermic process and downward an endothermic one.

Table 2
Area of DSC curve peaks

Sample	Endothermic peak (J/g)	Exothermic peak (J/g)
HF7	384	-32
LF7	279	-28
OF7	230	-28
EF7	274	-39

samples. Evolution of the values with the nature of the sample is inverse to the one of the mass change in the second TGA step: the larger the loss the smaller the enthalpy. This behavior is coherent with the assumption that it corresponds to the same process, in all the cases, but different amounts of reactants are involved.

For a better understanding of the decomposition processes, TPD analysis was performed in a flow of

He, flow rate $1 \text{ cm}^3 \text{ s}^{-1}$. The analysis of the gases evolved from TPD experiments was carried out by mass spectrometry, with a VG Spectralab SC 200, interfaced to a PC microcomputer. The experimental device of TPD-MS has been described elsewhere [7]. Eight m/e ratios from 12 to 44, chosen according to the expected outcome, were recorded. Signals for $m/e = 18, 17$ and 16 allow checking of the ammonium hydroxide and water, $m/e = 44$ and 12 for CO_2 , $m/e = 32$ for oxygen and $m/e = 30$ and 28 give information about NO. Fig. 3 presents the data corresponding to some of the ratios recorded for the sonogel LF7.

During the step at 100°C , the main residues in the evolved gases are water from the release of the water adsorbed at the surface of these strongly hydrophilic samples, and ammonia, from the formamide hydrolysis. The corresponding energy consumption is not vis-

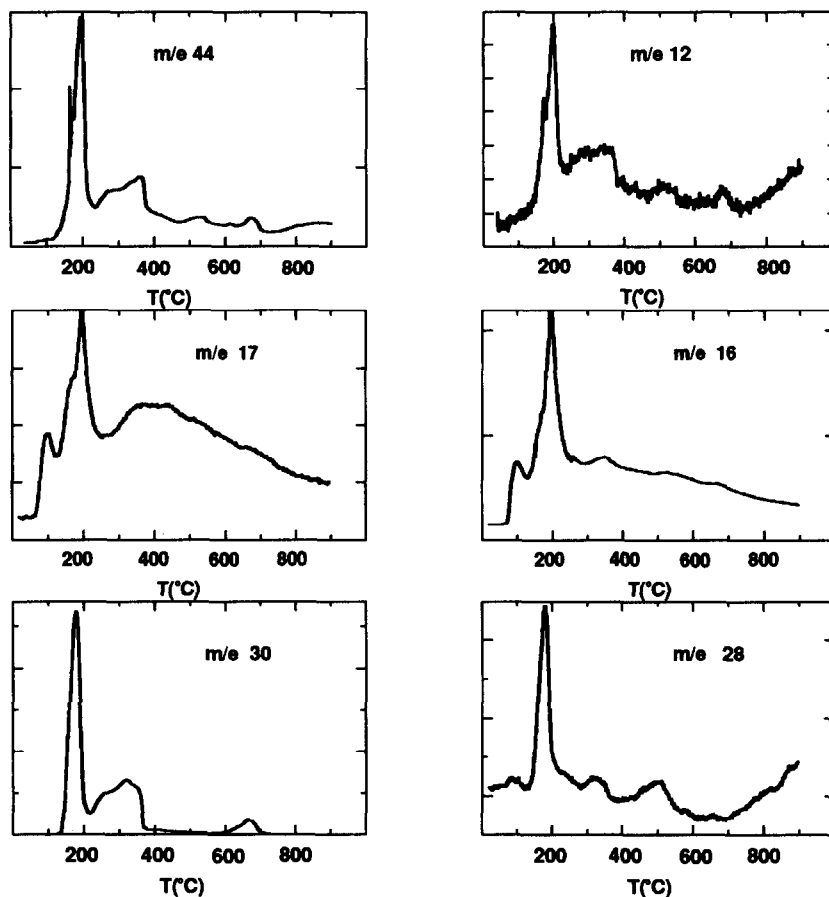


Fig. 3. Intensity of evolved gases of the LF7 sample as a function of temperature of m/e , representative ratios of the groups described in the text, by TPD.

ible from the DSC diagrams because they were registered after stabilization of the samples at 60°C for a certain time.

The endothermic process associated with the aforementioned TGA shoulder can be noticed as a shoulder at the 17 and 16 patterns (which can be assigned to the NH_3 and H_2O “fragmentation maps”) and the 44 and 12 patterns (corresponding to CO_2 traces).

4. Discussion

Desorption of hydrogen-bonded formamide is the main process that must be taken into consideration in order to explain the source of the composition of the residues of the He flow. Orcel et al. [8] have proposed that formamide is linked to the silica network as hydrogen-bonded by the $-\text{NH}_2$ group. This group is desorbed before $T=170^\circ\text{C}$ is reached and only the oxidation products are kept at the gel surface. In this way, we can assume that formamide desorption is followed by decomposition and oxidation processes which lead to CO_2 , NH_3 and H_2O formation with a final endothermic energy balance. A schematic description of the whole process is represented in Fig. 4. That means that the amplitude of the second TGA step is related to the amount of hydrogen-bonded formamide desorbed.

On the other hand, the occurrence of the oxidation reaction in the He flow can be justified by the presence

of air in the sample pores as well as the decrease of the remaining oxygen ($m/e=32$) traces [9]. This assumption is in agreement with the previous remark that the calculated enthalpies can be assigned to the same process in all the samples.

At 200°C a very intense signal is observed in all the checked TPD patterns as well as a mass loss during the third TGA step. Nevertheless, no peak was found at this temperature in the calorimetry or DTA experiments of any sample. Consequently, the outgoing products, responsible for the thermal features at this temperature, are presumably vapour coming from initially closed pores that open at this temperature without energy consumption.

The TGA step at 290°C must be related to the exothermic peak in the DTA and DSC curves. At this temperature, peaks at the TPD 44, 12 and 30, 28 patterns, related to CO_2 and NO residues, are also noticed. These gases are the oxidation products that were chemisorbed to the silica xerogel surface. In this case, the non-correlation between enthalpy and mass loss values indicates that organic residues are not the same for all the xerogels. Nevertheless, as should be expected, the remaining organic groups are more abundant in classic xerogels.

The last weight loss is presented in a widespread (300–800°C) temperature range at the TGA curve. A corresponding peak is observed in the TPD plots but is not in the DTA nor DSC curve. Thermal loss in this

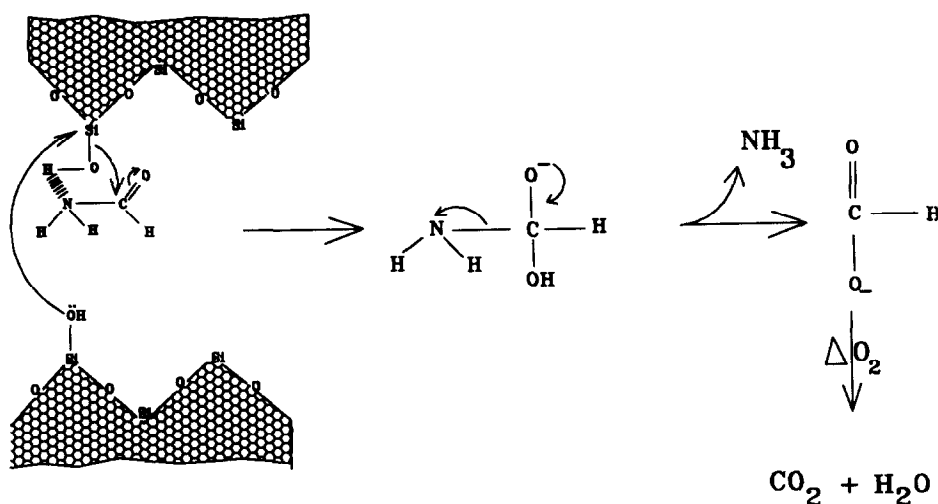


Fig. 4. Schematic description of the desorption–decomposition process of the hydrogen-bonded formamide at 170°C from which an endothermic energy balance and O_2 consumption result.

range can be assigned mainly to water and carbon dioxide. Water evolved in this step is produced by additional polycondensation of the silica network by means of the surface –OH group. When this process takes place in closed pores, “bloating” of the samples is known to occur during sintering. Therefore, when the goal of the processing is to obtain a monolithic and completely dense glass, the thermal history of the samples must be directed to the complete elimination of these groups before the final densification steps.

5. Conclusions

Formamide hydrogen-bonded to silica –OH surface has been proved to decompose at temperatures around 170°C. Experiments indicate that a higher amount of hydrogen-bonded formamide protecting the gel surface is present in sonogels. It has also been shown that, for the temperature range examined, the different analyses do not reveal substantial differences regarding the thermal evolution features.

Thermal analysis study leads to the consideration of three main temperature ranges in which the three processes of the gel thermal evolution take place. This analysis allows a sintering processing path of these samples to be designed in order to obtain monolithic pieces for specific applications.

Acknowledgement

The authors are indebted to Junta de Andalucía and Comisión Interministerial de Ciencia y Tecnología (Project MAT-91 1022) for financial support.

References

- [1] C.J. Brinker and G.W. Scherer, *Sol-gel science* (Academic Press, New York, 1990).
- [2] J. Zarzycki, M. Prassas and J. Phalippou, *J. Mater. Sci.* 17 (1982) 3371.
- [3] L.L. Hench, in: *Science of ceramic chemical processing*, eds. L.L. Hench and D.R. Ulrich (Wiley, New York, 1986) p. 52.
- [4] N. de la Rosa-Fox, L. Esquivias and J. Zarzycki, *Diffusion Defect Data* 53&54 (1987) 636.
- [5] N. de la Rosa-Fox, L. Esquivias and J. Zarzycki, *J. Mater. Sci. Letters* 10 (1991) 1237.
- [6] E. Blanco, N. de la Rosa-Fox and L. Esquivias, in: *Trends in non-crystalline solids*, eds. A. Conde, C.F. Conde and M. Millan (World Sci. Publ., Singapore, 1992) p. 69.
- [7] S. Bernal, R. García and J.M. Rodríguez-Izquierdo, *Termochim. Acta* 70 (1983) 249.
- [8] G. Orce, J. Phalippou and L. Hench, *J. Non-Cryst. Solids* 104 (1988) 170.
- [9] L. Esquivias, C. Fernández-Lorenzo and J.M. Rodríguez-Izquierdo, *Riv. della Staz. Sper. Vetro* 5 (1990) 85.